

Review

# New Materials and Technologies for Durability and Conservation of Building Heritage

Luigi Coppola <sup>1,\*</sup>, Tiziano Bellezze <sup>2</sup>, Alberto Belli <sup>3</sup>, Alessandra Bianco <sup>4</sup>, Elisa Blasi <sup>2</sup>, Miriam Cappello <sup>5</sup>, Domenico Caputo <sup>6</sup>, Mehdi Chougan <sup>4</sup>, Denny Coffetti <sup>1</sup>, Bartolomeo Coppola <sup>3</sup>, Valeria Corinaldesi <sup>2</sup>, Alberto D'Amore <sup>7</sup>, Valeria Daniele <sup>8</sup>, Luciano Di Maio <sup>9</sup>, Luca Di Palma <sup>10</sup>, Jacopo Donnini <sup>2</sup>, Giuseppe Ferrara <sup>3</sup>, Sara Filippi <sup>5</sup>, Matteo Gastaldi <sup>11</sup>, Nicola Generosi <sup>2</sup>, Chiara Giosuè <sup>2</sup>, Loredana Incarnato <sup>9</sup>, Francesca Lamastra <sup>4</sup>, Barbara Liguori <sup>6</sup>, Ludovico Macera <sup>8</sup>, Qaisar Maqbool <sup>2</sup>, Maria Cristina Mascolo <sup>12</sup>, Letterio Mavilia <sup>13</sup>, Alida Mazzoli <sup>2</sup>, Franco Medici <sup>10</sup>, Alessandra Mobili <sup>2</sup>, Giampiero Montesperelli <sup>4</sup>, Giorgio Pia <sup>14</sup>, Elena Redaelli <sup>11</sup>, Maria Letizia Ruello <sup>2</sup>, Paola Scarfato <sup>9</sup>, Giuliana Taglieri <sup>8</sup>, Francesca Tittarelli <sup>2</sup>, Jean-Marc Tulliani <sup>3</sup> and Antonino Valenza <sup>15</sup>

- <sup>1</sup> Department of Engineering and Applied Sciences, University of Bergamo, INSTM R.U., 24044 Dalmine, Italy
  - <sup>2</sup> Department of Materials, Environmental Sciences and Urban Planning, Università Politecnica delle Marche, INSTM R.U., 60131 Ancona, Italy
  - <sup>3</sup> Lince Laboratory, Department of Applied Science and Technology, Politecnico di Torino, INSTM R.U., 10129 Turin, Italy
  - <sup>4</sup> Department of Enterprise Engineering “Mario Lucertini”, University of Roma “Tor Vergata”, INSTM R.U., 00133 Rome, Italy
  - <sup>5</sup> Department of Civil and Industrial Engineering, University of Pisa, 56122 Pisa, Italy
  - <sup>6</sup> Department of Chemical, Materials and Industrial Engineering, University of Naples Federico II, 80125 Napoli, Italy
  - <sup>7</sup> Department of Engineering, University of Campania “Luigi Vanvitelli”, 81031 Aversa, Italy
  - <sup>8</sup> Department of Industrial and Information Engineering and Economics, University of L’Aquila, 67100 L’Aquila, Italy
  - <sup>9</sup> Department of Industrial Engineering, University of Salerno, 84084 Fisciano, Italy
  - <sup>10</sup> Department of Chemical Engineering Materials & Environment, Sapienza University of Rome, 00184 Rome, Italy
  - <sup>11</sup> Department of Chemistry, Materials and Chemical Engineering “G. Natta”, Politecnico di Milano, 20133 Milano, Italy
  - <sup>12</sup> Department of Civil and Mechanical Engineering, University of Cassino and Lazio Meridionale, 03043 Cassino, Italy
  - <sup>13</sup> Department of Heritage-Architecture-Urbanism, University of Reggio Calabria “Mediterranea”, 89124 Reggio Calabria, Italy
  - <sup>14</sup> Department of Mechanical, Chemical and Materials Engineering, University of Cagliari, 09123 Cagliari, Italy
  - <sup>15</sup> Department of Engineering, University of Palermo, 90123 Palermo, Italy
- \* Correspondence: luigi.coppola@unibg.it



**Citation:** Coppola, L.; Bellezze, T.; Belli, A.; Bianco, A.; Blasi, E.; Cappello, M.; Caputo, D.; Chougan, M.; Coffetti, D.; Coppola, B.; et al. New Materials and Technologies for Durability and Conservation of Building Heritage. *Materials* **2023**, *16*, 1190. <https://doi.org/10.3390/ma16031190>

Academic Editors: Paulo Santos and Rui Miguel Novais

Received: 18 November 2022

Revised: 12 January 2023

Accepted: 27 January 2023

Published: 30 January 2023



**Copyright:** © 2023 by the authors. Licensee MDPI, Basel, Switzerland. This article is an open access article distributed under the terms and conditions of the Creative Commons Attribution (CC BY) license (<https://creativecommons.org/licenses/by/4.0/>).

**Abstract:** The increase in concrete structures’ durability is a milestone to improve the sustainability of buildings and infrastructures. In order to ensure a prolonged service life, it is necessary to detect the deterioration of materials by means of monitoring systems aimed at evaluating not only the penetration of aggressive substances into concrete but also the corrosion of carbon-steel reinforcement. Therefore, proper data collection makes it possible to plan suitable restoration works which can be carried out with traditional or innovative techniques and materials. This work focuses on building heritage and it highlights the most recent findings for the conservation and restoration of reinforced concrete structures and masonry buildings.

**Keywords:** durability; concrete structures; sustainability; new materials

## 1. Introduction

The construction sector depletes 40% of the planet's energy resources [1,2]. To decrease the energy consumption of buildings in order to improve their sustainability, a key aspect to consider is the durability of concrete structures (such as buildings, tunnels and bridges), since it highly affects their service life [3].

The durability of concrete is strongly influenced by the interactions between concrete itself and the surrounding environment, which is rich in contaminants [4]. Among several causes, the most common are water penetration, since water represents the main carrier of aggressive agents [5–7]; CO<sub>2</sub> penetration, which determines cement matrix carbonation and, in presence of moist air, is responsible for reinforcement corrosion [8]; chloride penetration, which initiates reinforcement corrosion [9]; heavy metal contact and incorporation; and fire development, which degrades the concrete itself [10].

From “The Law of Fives” by De Sitter (Figure 1), it is well known that the costs of repairing a concrete structure grow exponentially if the works are done long after the first damage appears, especially in the case of reinforced-concrete-based monuments [11]. Therefore, it becomes clear that monitoring the penetration of aggressive agents in concrete is important to accelerate interventions, which can in turn reduce maintenance costs and increase the structural safety of structures [12]. Additionally, the Italian Technical Regulations for Buildings (approved on 17 January 2018) reports in its Chapter 2 “Safety and Expected Performance” that an adequate level of durability can be guaranteed by adopting passive and active control systems.

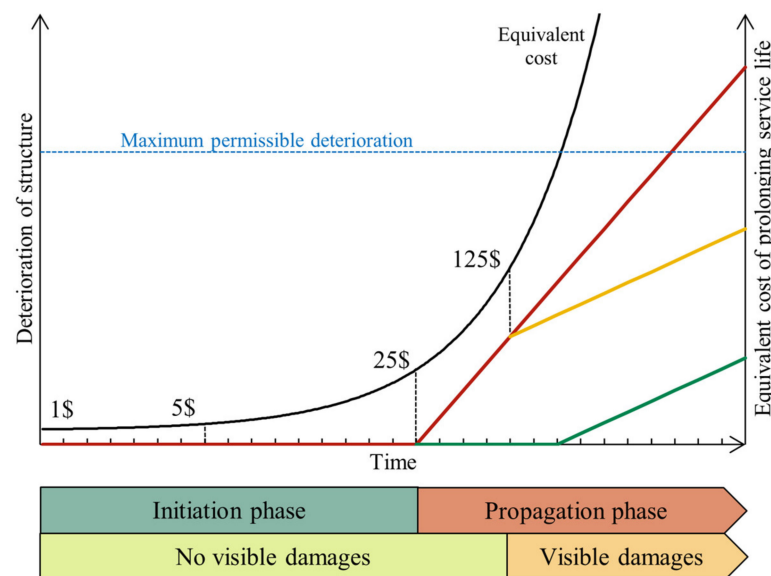


**Figure 1.** De Sitter's "Law of Fives" in Tuutti's diagram. Re-elaborated from [11,13].

The purpose of this review is to analyze the latest findings on materials and techniques devoted to ensuring prolonged durability and proper conservation of reinforced-concrete-based heritage.

## 2. Monitoring Systems for Durable Concrete Structures

The diagnosis of durability should take place through a methodological path primarily based on the visual analysis of the structure to detect possible visible degradation phenomena and on the acquisition of historical–geographic data. These data are complementary to the results obtained by in situ and laboratory tests to assess the diagnosis and to define the maintenance interventions to be carried out.

On one hand, the main destructive tests performed on samples extracted from the structure and analyzed in laboratory include the chemical (chromatography, X-ray diffraction, thermal analysis, FT-IR spectroscopy), physical (mercury intrusion porosimetry),

morphological (optical and electronic microscopy) and elasto-mechanical (modulus of elasticity, compressive and tensile strength, etc.) characterization of materials.

On the other hand, on-site non-destructive tests, mainly focused on elastic–mechanical characteristics of the concrete, are endoscopy, sclerometry, thermography, pull out, and sonic and ultrasonic investigations. Colorimetric methodologies [14] are used to detect the penetration depth of CO<sub>2</sub> and chlorides, whereas potential mapping and resistivity measurements are used to monitor reinforcement corrosion.

However, continuously monitoring selected parameters through embedded probes, in order to detect the initiation of degradation as early as possible, can further decrease costs and improve the safety of structures, because it increases the chance of detecting any significant variation of the chosen parameter related to a degradation process. Therefore, numerous probes to be embedded in concrete have been developed, such as electrical resistance probes (ERP) [15], macro-couple probes, pseudo reference electrodes to measure free corrosion potential (activated Ti mixed metal oxide (MMO), Zn) and multi-parametric sensors [16].

In particular, the free corrosion potential is easy to measure and can be used to control the durability of reinforced concrete structures, since it is sensitive not only to the corrosive state of the reinforcements but also to the water saturation degree of the concrete between the monitored reinforcement and the embedded probe. It is worthy to underline that water is the main factor influencing the durability of structures, since it transports the main aggressive agents and it is the medium in which deterioration reactions take place. A continuous monitoring system for preventive and planned maintenance of structures based on simple measurement of the free corrosion potential has been already proposed (i.e., CoSMoNet [17], Figure 2) and successfully applied to several concrete structures. The system provides signals, revealed by embedded electrodes and sent to a peripheral device for remote reading, where data are suitably analyzed and stored and finally sent to a monitoring station for their processing. Special alerts are arranged when the variation in the measured values exceeds a maximum threshold previously established. In this way, a continuous monitoring of different reinforced concrete structures located everywhere in the world can be carried out from the same monitoring station.



Figure 2. The Co.S.Mo.Net monitoring system.

The most recently proposed advanced non-destructive testing tools and procedures for structural health monitoring (SHM) are sensorized non-metallic reinforcement systems for concrete [18], computer vision [19], also combined with thermography [20,21], and

electrical resistivity [22] (i.e., EU Project: EnDurCrete [23]). Electrical resistivity, which can be determined by electrochemical impedance spectroscopy (EIS), is getting much attention compared with other methods. Indeed, the EIS characteristics make it possible to exploit the self-sensing capability of concrete, which means its ability to sense its own condition (e.g., cracks, water penetration, strain) [24]. This ability can be enhanced by increasing the electrical conductivity of concrete by adding conductive materials such as fillers/fibers [25–27]; higher concrete conductivity allows the monitoring of concrete structures by means of low-cost instrumentation given the higher signal-to-noise ratio (SNR) that can be obtained [28]. Concerning fillers, carbon nanotubes [29], graphene [30], carbon black [31,32], and nickel powder [33] have been proven to increase the electrical conductivity of mortars/concretes besides their mechanical performance and durability [34–36]. Concerning fibers, Xie et al. [37] focused on the relationship between fiber content and electrical conductivity of the cement-based composite, highlighting a remarkable reduction in the electrical resistivity if the fiber content is higher than a threshold due to the increase in electrical contact paths between the fibers. Comparing steel and carbon fibers [38], a recently published work has shown the best effectiveness is in recycled carbon fibers (RCF) compared with virgin carbon fibers (VCF) and brass-coated fibers (BSF) in noticeably reducing concrete resistivity even at low fiber dosages [39]. This result can be ascribed to the high number of carbon micro-particles on the fibers' surface, which increase the specific conductive surface of RCF [40].

### 3. Sensors to Evaluate the Carbonation of Concrete

Carbonation is a two-step reaction process between: (i) atmospheric CO<sub>2</sub> (about 419 ppm by volume in December 2022, measured at the Mauna Loa Observatory in Hawaii, USA [41]) with water present in concrete capillary pores which leads to the formation of carbonic acid (H<sub>2</sub>CO<sub>3</sub>) and (ii), by reaction of H<sub>2</sub>CO<sub>3</sub> with calcium compounds (primarily, portlandite (Ca(OH)<sub>2</sub>)), to produce calcium carbonate (CaCO<sub>3</sub>) and water. The decrease in the portlandite concentration reduces the pH of the pore solution to a value of about 8.3 after complete carbonation of concrete [42]. However, reinforced concrete structures require a high pH to maintain the stability of the passivated layer on top of the rebars. When the pH value decreases, this protective oxide layer breaks and corrosion can occur. In addition, the corrosion is accelerated if the steel rebars are exposed to aggressive agents such as chloride ions. The corrosion produces expansive iron oxides/hydroxides and causes, in hardened concrete, internal tensile stresses, cracking and spalling of the concrete cover. Exposure conditions, in particular relative humidity (RH), play a fundamental role in the carbonation depth and the amount of CO<sub>2</sub> reacted over time, as carbonation is favored in the RH value range from 40 to 90% [42]. The carbonation rate is also influenced by the mix design of concrete (type and dosage of cement, water-to-cement ratio and, thus, porosity of concrete), as well as curing conditions. In most structures made using good-quality concrete, carbonation needs many years to extend as far as the depth of the rebars [43].

The most common method for the evaluation of carbonation is destructive and involves a 1% (*w/v*) solution of phenolphthalein in ethanol, usually sprayed on cylindrical samples cored from concrete structures [44]. This pH indicator varies its color from pink/purple (in a non-carbonated environment) to colorless when the pH value is below 9.0–9.5, evidencing the carbonated area. Sensors working in accordance with electrochemical principles, like potential, polarization resistance and electrochemical impedance measurements [45], fiber-optic sensors based on Fabry–Perot interferometer strain sensors [46] or acoustic emission [47] are also used to assess the corrosion rate of rebars in reinforced concrete structures. However, these sensors are placed in direct contact with steel reinforcements and can alert only after the initiation of the corrosion process, which is in most cases already too late. Thus, preventing rebar damage and early detection of the carbonation depth of a concrete cover before rebars are reached is of paramount importance. A state-of-the-art pH determination in hardened concrete was published by

Behnood et al. [48], where destructive (based on pore solution extraction/leaching) and non-destructive (with embedded sensors) approaches were deeply illustrated.

Even if potentiometric sensors for pH measurement are commonly used in many areas, their use to monitor the pH of concrete pore solution is somewhat limited [49]. Iridium/iridium oxide ( $\text{IrO}_x$ ) electrodes [50–53] and screen-printed Ag/Ag<sub>2</sub>O [53] or IrO<sub>x</sub> [54] sensors were studied with this aim.

Electrode pH probes to monitor pH evolution at different depths were also investigated. For example, a fiber-optic sensor based on a pH-sensitive layer entrapping a pH indicator which changed color in response to the carbonation state of the cementitious matrix was described by Habel and Krebber [55]. Other papers also illustrated the interest in using sol-gel optic fiber sensors for pH monitoring in cementitious materials [56–58]. McPolin et al. produced by a sol-gel method an optic fiber probe with a cresol-red indicator dye trapped inside (pH variation between 8 and 13), embedded it in cement mortar samples, and monitored pH changes over 18 months [59]. Khalil et al. presented a pH sensor based on meso-tetraarylporpholactone, which shifted color in the 11.5–13.2 pH range [60]. Srinivasan et al. used a sol-gel/TNBS (trinitrobenzenesulfonic acid) composite that showed a variation in color in the pH range from 12 to 14 [61]. Finally, Inserra et al. [62] developed an optical pH probe with a pH-sensitive dye embedded in a silica monolith made by a sol-gel method. Alizarin yellow, which changes color from yellow to red when the pH ranges from 10 to 12, was used for this purpose.

#### 4. Electrochemical Techniques for Repairing Reinforced Concrete Structures

In some cases, specifically when concrete damage is due to reinforcement corrosion, conventional repair techniques may not be enough to guarantee the required service life of the intervention. For instance, this may be related to the inadequacy of concrete cover thickness, high aggressiveness of the environment, or the need to remove large quantities of structurally sound concrete. In such cases, electrochemical techniques can be an advantageous option, since they can interrupt corrosion propagation, leaving the concrete in place, provided it has not been damaged yet.

Electrochemical techniques can be permanent or temporary [63–66]. The main permanent technique is cathodic protection, which is based on the application of a small current density (up to a few tens of mA/m<sup>2</sup>) to protect steel reinforcement. Re-alkalisation and chloride removal are temporary treatments that rely on the application of a much higher current density (up to few A/m<sup>2</sup>) for several weeks or a few months to change concrete's composition and restore its ability to protect the reinforcement.

All techniques rely on the application of a cathodic current to the reinforcement, usually supplied by a metallic anode placed on the concrete surface (for cathodic protection, the anode is embedded in a layer of mortar, while for temporary techniques the anode is embedded in cellulose pulp and removed at the end of the treatment). The main effect of the current is a reduction in steel potential, and a subsequent reduction in the corrosion rate. This effect is temporary (it is lost if the current is switched off); as long as the current is circulating, the rate of the anodic reaction (oxidation of iron) is depressed and the rate of the cathodic reaction (production of OH<sup>-</sup>) is increased. If very negative potential values are reached, the cathodic reaction of hydrogen evolution can also occur, and its consequences should be carefully evaluated in the case of high-strength steel bars in prestressed concrete structures [67,68].

The applied current also changes the properties of the concrete. The already mentioned production of alkalinity increases the pH at the steel–concrete interface, strengthening the protection so that short interruptions of the applied current can be tolerated. Moreover, the movement of anions in opposite directions to the current spreads alkalinity over larger areas of concrete and takes chlorides away from the rebar. These effects are beneficial, but marginal, in the case of cathodic protection; conversely, they are of primary importance for temporary treatments.



All electrochemical techniques need monitoring to check that the current is flowing and it is enough to protect the reinforcement (this also applies to re-alkalisation and chloride removal, where, in addition, monitoring of the corrosion conditions of the rebar after the treatment is advisable) [69].

Traditionally, cathodic protection is applied to structures suffering chloride-induced corrosion, typically slabs of bridges and viaducts or marine structures; however, it can be conveniently applied to carbonated concrete as well. The use of sacrificial anodes is also possible, by inserting discrete elements of zinc into the concrete and connecting them to the rebars (in this case, the duration is limited by the consumption of the anode material) [70–72].

Temporary treatments are used when it is not possible to apply a permanent anode, either for technical or aesthetical requirements. They can be used on complex shapes (e.g., statues) or if the texture of the surface cannot be changed (e.g., fair-faced concrete). Their effectiveness is more limited in time, and also because the cause of corrosion (e.g., carbonation or chloride penetration) continues after the treatment; it is also reduced if corrosion products are abundant at the steel–concrete interface [73–75].

## 5. Multi-Functional Graphene-Based Cement Composites for Durable Repaired Structures

In the last decade, graphene-based cement composites (GBCCs) have been strongly investigated due to their enhanced mechanical properties, often combined with smart properties (such as electrical, thermal, piezoresistive and electromagnetic properties), fire resistance and freeze-thaw resistance [76]. Moreover, very recently, it has also been proved that GBCCs show reduced permeability and chloride penetration. Several novel applications are expected in the near future for graphene-based cement nanocomposites as smart repair materials in the fields of offshore structures, geothermal piles, radiant systems, smart pavements, deicing roads and electromagnetic shielding [77–79].

The family of graphene-based materials (GBMs) is wide and includes several nanomaterials, classified on the basis of three key parameters: number of graphene layers, average lateral size and C/O atomic ratio [80].

A number of different characterization techniques are thus needed to fully characterize GBMs, such as Raman spectroscopy, infrared (IR) spectroscopy, X-ray photoelectron spectroscopy (XPS), and X-ray diffraction (XRD) combined with an extensive investigation by means of scanning electron microscopy (SEM), transmission electron microscopy (TEM) and atomic force microscopy (AFM) [81]. Recently, inelastic neutron scattering has been used to assess the hydration of GBCCs and the interactions between fillers, additives and hydrated cement phases [82].

One of the main issues with graphene-based materials is the workability of the fresh mortars, which is severely dependent on both the type and amount of the loaded GBMs. Usually, due to the tendency of these nanofillers to absorb water molecules, the flowability of GBM-modified cementitious admixtures is reduced; the extent depends on several different parameters, but mostly on the C/O ratio [83]. Furthermore, a good interaction between carbonaceous filler and matrix is mandatory to enhance the mechanical and functional properties of the composites. In fact, these fillers have often a strong tendency to agglomerate under attractive forces (e.g., Van der Waals), hindering the positive effect of the filler. The use of a natural rubber latex aqueous dispersion has been exploited to avoid the confinement of multiwall carbon nanotubes (MWCNTs) and reduced graphene oxide (rGO) in the production of multifunctional cement mortars with enhanced piezoresistive properties [82]. This new approach makes possible either avoiding filler aggregation or obtaining a three-dimensional network with fillers located on the single latex particles in a continuous rubbery phase.

Analogously, scientists involved in this adventurous field are aware that the mechanical and physical properties of hardened graphene-based cement nanocomposites strictly depend on the selection of type (i.e., size, composition, thickness, roughness, dispersibil-

ity, . . .) and dosage (usually between 0.01% and 1% by weight of cement) of the loaded graphene-based materials [84]. For this reason, although in the literature the great potential of these graphene-based cement composites has been fully assessed, the results in terms of final mechanical and physical properties are still unpredictable. Presently, most studies on GBCCs have been focused on cements and mortars. For example, cementitious composites filled with multi-layer graphenes (MLGs) showed a 54% increase in compressive strength and a 21% reinforcement in flexural strength, mainly attributed to extensive and strong bonding between the nanofiller and the matrix combined with the lowered orientation index of portlandite crystals [85]. Moreover, GBCCs also demonstrated a reduced chloride ion diffusion, associated with improved hydrophobicity, accelerated hydration kinetics and enhanced densification of the manufactures [26]. Recently, several papers have focused on the effect of GBMs in mortars or concrete on the diffusion of  $\text{Cl}^-$  ions in cementitious matrix [86,87]. Du and Pang [88] showed that the addition of 1.5% by weight of cement of such nanofillers in concrete promotes a decrease in chloride depth ranging from 60 to 70% relative to plain concrete. Similarly, Dimov et al. [89] published an outstanding, extensive paper on graphene-modified concrete. The authors clearly demonstrated an increase of up to 146% in the compressive and 79.5% in the flexural strength, combined with enhanced electrical and thermal conductivity; moreover, the graphene-modified concrete showed nearly 400% decreased water permeability. These results definitely open up the emerging field of multifunctional nanoengineered concrete for a more sustainable construction industry.

Obviously, safety, costs and life cycle assessment (LCA) should be rigorously evaluated for large-scale applications [90,91].

## 6. Inorganic Matrix Composite Systems for the Repair and Strengthening of Existing Structures

The development of new inorganic matrix composite systems with strong mechanical performance has introduced into the construction industry new potential tools to repair and improve both the resistance and durability of existing concrete and masonry structures [92–94]. The advantages of using these systems, relative to more traditional ones, lie in their high strength/weight ratio, ease of application, greater compatibility with the substrate and better resistance to high temperatures and fire exposure. Within this new class of inorganic-based materials, those that have been developed and spread more in the construction sector are FRCM (fabric-reinforced cementitious matrix), CRM (composite reinforced mortar) and UHPFRC (ultra-high-performance fiber-reinforced concrete), Figure 3.

FRCM systems consist of an inorganic matrix (usually cement or lime-based mortar) reinforced with fabrics in the form of open grids (made of carbon, glass, basalt or PBO fibers). These systems, which have a thickness of between 10 and 15 mm, are specifically designed to be applied as external reinforcements on existing masonry or concrete structures (Figure 3a–c). As compared with more traditional strengthening solutions, such as steel-reinforced concrete plasters, FRCMs are more durable, since they have no problems related to the corrosion of the internal reinforcement and they offer better efficiency in terms of resistance/weight, as well as reversibility of the intervention and ease of application.

In recent years, the scientific community has paid great attention to this new class of composite materials, and some guidelines giving instructions on how to design a strengthening intervention with FRCM have been provided by the American Concrete Institute (ACI 549.4R-13) and Italian CNR (DT215/2018) [95,96], while acceptance criteria and indications of characterization methods are given by the ICC Evaluation Service (AC434.13), the Italian CSLLPP, and Rilem TC 250 [97–99]. Several studies have focused on the mechanical characterization of FRCM [100], on the bond at the interface between the internal reinforcement and the inorganic matrix [101–103] and on the effectiveness of different FRCM systems to repair and strengthen masonry or concrete elements [104–108]. There are still other issues to be further investigated, such as the long-term behavior and durability of FRCM systems when exposed to aggressive environments [109–113], high temperature or fire scenarios [114,115].

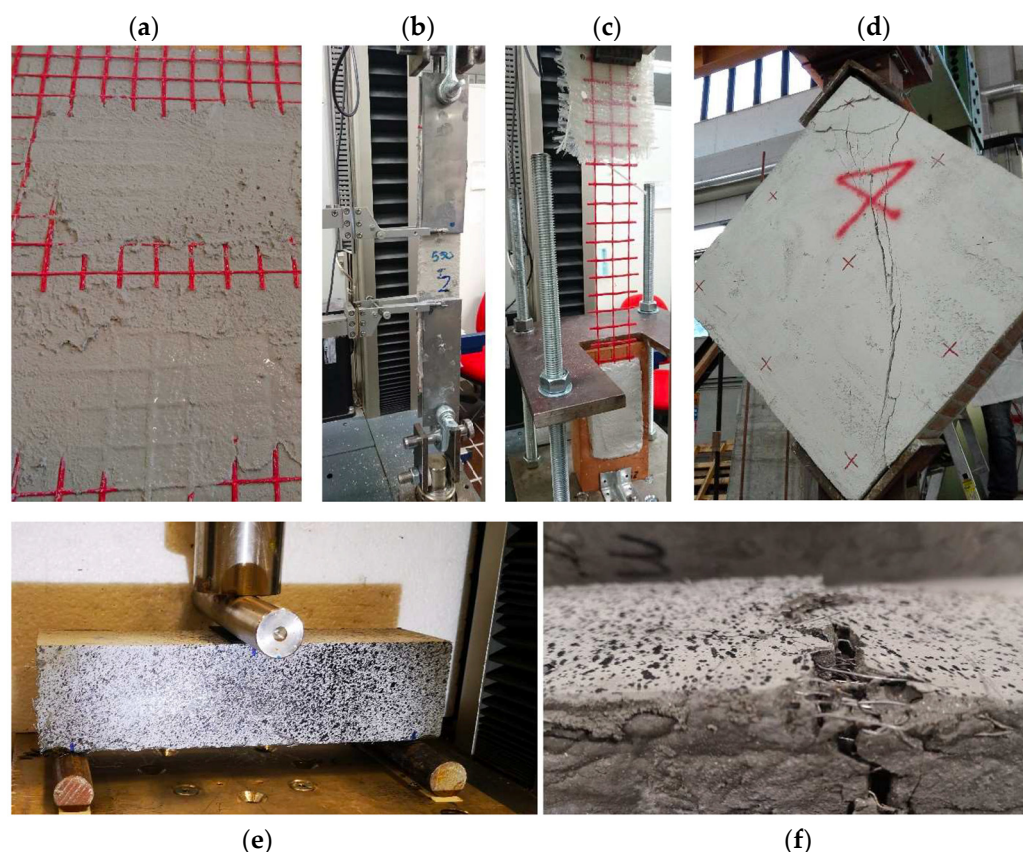


**Figure 3.** Inorganic matrix composite systems: (a) FRCM made of glass fabric and cementitious mortar; (b,c) mechanical characterization tests of FRCM systems; (d) diagonal compression test on masonry reinforced with CRM; (e,f) three-point bending test on a UHPFRC specimen and detail of the steel fibers after cracking.

CRM systems are made of a pre-impregnated composite mesh (FRP) embedded within inorganic mortar (usually lime-based) with a compressive strength between 5 and 20 MPa. In these systems, the FRP mesh bears the tensile stresses, while the structural mortar is responsible for the stress transfer between the composite grid and the substrate. The transfer of stresses between the support to be reinforced and the reinforcement mesh is also guaranteed by the presence of connectors, which ensure the structural collaboration between the wall element and the reinforced plaster. The total thickness of CRM systems is usually between 30 mm and 50 mm. The most-used fibers are made of AR glass, carbon or basalt, coated with a thermosetting polymer matrix. These systems have had strong development in the last 5 years and a high diffusion especially into the Italian construction market. Further spread of these systems has also been facilitated by the recent technical guidelines for identification, qualification and acceptance control of CRM issued by the Italian CSLPP [116].

Although recently introduced, CRM showed promising results in improving the mechanical performance of different masonry structures, such as walls and arches [117–119]. Reinforcement can be applied on one side only or on both sides of the masonry (Figure 3d). Diagonal compression tests on masonry walls showed an increase of the shear capacity from 42% to 85% for a single-sided configuration and from 138% up to 288% in a double-sided configuration, relative to unreinforced masonry panels [120].

UHPFRCs are advanced cementitious materials with excellent mechanical properties: they can achieve compressive strength greater than 150 MPa, flexural strength higher than 40 MPa and considerable tensile-strain-hardening behavior [121,122]. Due to their superior properties, UHPFRCs are being increasingly used to produce thin and extremely resistant structural components [123,124] or as overlay systems to repair existing concrete



elements such as pillars, beams and slabs (Figure 3e,f) and to improve their mechanical performance and durability properties [125–128]. UHPFRC mixtures are characterized by a significant amount of cement ( $>600 \text{ kg/m}^3$ ), small size aggregates ( $<6 \text{ mm}$ ), binders (fly ash, silica fume, reactive powder), superplasticizers and a low water/cement ratio ( $w/c < 0.2$ ). Steel fibers (length of  $10 \div 20 \text{ mm}$ ) are usually added with a dosage of about 2–3% by volume to significantly improve tensile strength and strain capacity [129–133]. A well-designed UHPFRC is able to exhibit, when subjected to uniaxial tensile strength, a strain-hardening behavior in the post-cracking phase. This phenomenon, observed by Wille et al. and Naaman and Reinhardt [121,122], is generally accompanied by the formation of multiple transversal cracks at different specimen cross-sections. For this reason, the tensile strength of these materials cannot be neglected during the design phase (as is the case of ordinary concrete). Some recommendations on how to perform direct tensile tests on UHPFRC materials have been provided by a few national guidelines, such as the French AFGC-SETRA [134] and the Japanese JSCE [135]. However, the complete mechanical characterization of UHPFRC (especially regarding its tensile strength) is still an open issue.

## 7. Fibrous and Particle Systems for Repairing Mortars

Different strategies can be used to avoid or to reduce structure degradation or to repair structures that are already damaged [136]. The use of fibrous and particle systems are two viable strategies to overcome most of the issues of cementitious structures. In particular, steel fibers or polymeric fibers with a high elastic modulus are mainly used in concrete to increase its fracture toughness and flexural post-cracking behaviour (Figure 4a). On the other side, randomly oriented polymeric fibers having a low elastic modulus are generally used into cementitious mortars to avoid shrinkage cracking phenomena (Figure 4b) [137,138]. Considering shrinkage cracking phenomena and mechanical property improvements, fiber amounts and shape (geometry, cross-section and surface texture) are the two most important parameters that should be taken into account. Fibers can dramatically decrease crack numbers and width without excessively compromising mortar's fresh properties. However, the interfacial transition zone (ITZ) between fibers and the cementitious matrix is crucial. To contrast cracking phenomena, polymeric fibers of different nature are generally used (in particular, PET, PA, PE and PP), with some recent innovations like nanocomposite polymeric fibers which have better mechanical properties compared with conventional polymeric fibers [139–142]. Indeed, most of the polymeric fibers are smooth and have weak adhesion with the matrix. Therefore, several strategies can be adopted to improve fiber/matrix adhesion: fiber surface roughness and geometry modification or improvement of the chemical affinity between fibers and the matrix [143,144]. Meanwhile, using natural fibers (hemp, flax, sisal, cellulose, bamboo etc.), there are more interactions between fibers and the matrix thanks to the interlocking positions offered by lumen and pores already present in natural fibers [145–148]. Moreover, material choice is also fundamental in terms of sustainability. Plastic fibers produced starting from recycled polymers should be preferred to virgin polymers, and natural fibers should be preferred to mineral fibers that are produced at high temperatures (e.g., basalt) [149–154]. Indeed, the reuse of wastes deriving from different streams (e.g., polymeric, sewage sludge, construction and demolition, etc.) is an effective strategy to improve the sustainability of the building and construction sector [155,156]. Some efforts have been made to extend the strong potential of plastic waste obtained by plasticization and densification of the polymeric fraction of municipal solid waste (MSW) in the field of lightweight concrete [157]. Satisfactory adhesion and good compatibility between plastic aggregates and a cement matrix were confirmed by SEM analysis (Figure 4). Even with a small amount of plastic substitution (about 10%), the concrete was compliant with Italian standards for structural use; a significant improvement in tensile strength can be achieved thanks to the fiber-like behavior of plastic waste [157].

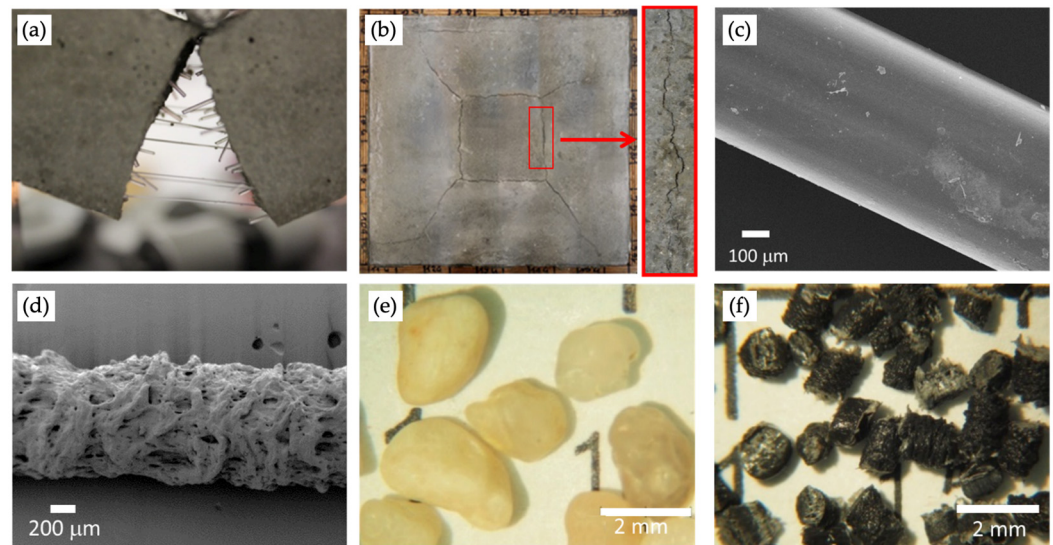


**Figure 4.** (a) Polymeric fibers bridging the two sides of a mortar sample after a flexural test; (b) shrinkage cracking phenomena occurring after an accelerated test; (c) FE-SEM micrograph of a smooth PP fiber; (d) FE-SEM micrograph of an engineered roughened fiber; (e) silica sand; and (f) artificial aggregates prepared using a secondary raw material.

A further improvement in terms of sustainability can derive from the substitution of traditional aggregates used for cementitious mortars with more innovative ones. Indeed, by varying the nature, the morphology and the chemical properties of the aggregates, several benefits can be obtained. As for fibers, aggregates can also be prepared starting from secondary raw materials [152,158,159]. Using porous and lightweight aggregates, it is possible to reduce the specific weight of the composite [158,160,161]. Moreover, porous aggregates can be saturated to be used as water reservoirs for internal curing or as carriers for self-healing agents [162,163]. Moreover, hygro-thermal properties can be improved by opportunely tuning aggregate amounts, reducing thermal conductivity and increasing water vapor permeability [159,164,165]. Finally, using plastic aggregates is also possible to improve the impact and shock resistance of cementitious mortars [166].

## 8. Nanolime-Based Formulations for the Conservation of Cultural Heritage

Silica fume (SF) and natural pozzolans (NP) have been widely used as substitutes for Portland cement (OPC) for concrete manufacturing, in relation to their advantageous properties, including reduced environmental impact, low heat of hydration, low water permeability, high chemical resistance and resistance against the alkali–silica reaction, improved fresh properties, low shrinkage and reduced cost [167,168]. In particular, in such cases, both SF and NP play a fundamental role in improving the packaging density of the solids, but their primary role is to provide additional calcium silicate hydrate (C-S-H) through reaction with water and the calcium hydroxide coming from the hydration of OPC [169–171].

The interaction, in terms of the production of C-S-H, between NP and SF and an aqueous suspension of nanolime particles (nCH) produced in the laboratory by means of a patented, eco-friendly and one-step synthetic route based on an ion-exchange process makes it possible to obtain large amounts of product [172–176]. The interaction between nCH and NP/SF is realized in water, working at room temperature, considering different nCH/NP and nCH/SF ratios, corresponding to 1:1 and 1:2 in weight, and a water/solid ratio (W/S) equal to 6. The obtained mixtures are analyzed at different aging times, from 30 min up to 120 days. Both the as-received commercial NP/SF and the synthesized nCH are characterized by means of several techniques, such as XRD, XRF and transmission electron microscopy (TEM) analyses. The produced mixtures are investigated in terms of the phase composition of the formed hydrates at different aging times. Scanning electron

microscopy (SEM) is used to investigate their morphological features as well. In addition, surface measurements (BET) are performed.

From XRF, SF is characterized by 94.82% SiO<sub>2</sub>, 0.79% Fe<sub>2</sub>O<sub>3</sub> and minor amounts of MgO, K<sub>2</sub>O, CaO and Al<sub>2</sub>O<sub>3</sub>, while the NP is composed of 69.17% SiO<sub>2</sub>, 1.16% TiO<sub>2</sub> and minor amounts of Al<sub>2</sub>O<sub>3</sub>, K<sub>2</sub>O, SO<sub>3</sub> and Fe<sub>2</sub>O<sub>3</sub>. BET analyses reveal surface area values of about 12.5 m<sup>2</sup>/g and 60 m<sup>2</sup>/g for SF and NP, respectively. The synthesized nCH appears pure and crystalline, in the form of hexagonal lamellas consisting of primary nanoparticles with dimensions ≤ 10 nm. Moreover, the aqueous suspensions of nCH show a high reactivity, guaranteeing a complete conversion into calcium carbonate, in the form of pure calcite, in a few hours, even in low-relative-humidity conditions [175]. As concerns the nCH/SF mixtures, from the XRD spectra the initial formation of C-S-H is evident after only 3 and 14 days of hydration, considering nCH/SF ratios of 1:2 and 1:1, respectively. In the sample characterized by a nCH/SF ratio of 1:2, after 14 days all the Ca(OH)<sub>2</sub> is consumed and the C-S-H formation proceeds in time appearing more crystalline, mainly in the C-S-H(I) form. The mixture with NP is characterized by a high reaction rate, especially at low hydration times, with the formation of C-S-H after only 1 day of aging. Nevertheless, the Ca(OH)<sub>2</sub> is not completely consumed up to 14 and 60 days, considering nCH/NP ratios of 1:2 and 1:1, respectively. The obtained results are very promising if compared with the literature data, which indicate a progressive reduction in free lime over time, leading to a total consumption at 90 and 365 days when silica fume or natural pozzolan are employed, respectively. Considering BET results, specific surface values of about 121 m<sup>2</sup>/g and 154 m<sup>2</sup>/g are obtained, referring to nCH/SF and nCH/NP mixtures with 1:2 ratios, respectively. Finally, SEM images of nCH/SF mixtures after 28 days of hydration show the formation of crumpled foils, with a thickness of few nanometers, characterized by the typical fibrous structure. In the nCH/NP mixtures, the formation of highly wrinkled layers covering all particles, constituted by marked crumple and rough-edge surfaces, is observed as well (Figure 5).

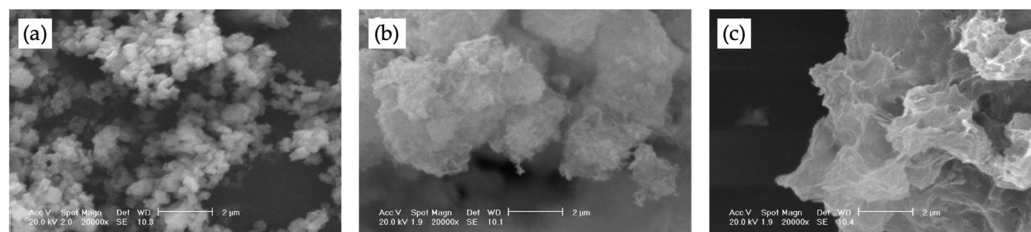


**Figure 5.** SEM images of nCH/NP mixtures at different hydration times: (a) after 30 min; (b) after 28 days, considering a nCH/NP ratio of 1:1; (c) after 28 days, considering a nCH/NP ratio of 1:2. Scale bar: 2 µm.

## 9. Future Trends

In the development of a conservative strategy for building heritage, evaluation of the state of conservation of the materials plays a central role. This survey is done using both monitoring techniques for the existing structures before the restoration work and evaluation of the effectiveness of the maintenance already carried out in the past. With the aim of a new conservation philosophy, all techniques, traditional or innovative, for acquiring information about the building's health conditions are fundamental, and also using strategies originally developed for other sectors (i.e., digital twins, artificial neural networks). Furthermore, the acquisition of data makes it possible to provide a large functional database for the development and refinement of the repairing materials and techniques of the future.

Therefore, starting from the knowledge of the building, the choice of traditional or innovative techniques will have to take into account, in addition to all the issues related to the quality of the restoration work, also sustainability, thus preferring the use of low-environmental-impact solutions (i.e., with low CO<sub>2</sub> emissions, limited consumption of energy and natural resources, reuse of waste products and use of recyclable materials)

capable of guaranteeing a prolonged service life for the building as discussed in a previous review by the authors [3].

## 10. Conclusions

This review highlights the most recent findings for the conservation and restoration of building heritage. In particular, it focuses on the need to guarantee a proper diagnosis of the durability of existing structures, and it shows that it is possible to preserve building heritage by using electrochemical techniques (when reinforced concrete elements are carbonated and/or in contact with chlorides). Moreover, some innovative techniques and materials for repairing building heritage (such as smart graphene-based materials, inorganic matrix composites, nano-limes and cementitious systems containing fibrous or particle reinforcements) are presented.

**Author Contributions:** Conceptualization: L.C. and D.C. (Denny Coffetti); Section 2: T.B., A.B. (Alberto Belli), E.B., C.G., A.M. (Alida Mazzoli), A.M. (Alessandra Mobili) and F.T.; Section 3: B.C., G.F. and J.-M.T.; Section 4: M.G. and E.R.; Section 5: A.B. (Alessandra Bianco), M.C. (Mehdi Chougan), F.L. and G.M.; Section 6: V.C., J.D., N.G., Q.M. and M.L.R.; Section 7: D.C. (Domenico Caputo), L.D.M., L.I., B.L. and P.S.; Section 8: V.D., L.M. (Ludovico Macera) and G.T.; writing—review and editing: M.C. (Miriam Cappello), A.D., L.D.P., S.F., M.C.M., L.M. (Letterio Mavilia), F.M., G.P. and A.V. All authors have read and agreed to the published version of the manuscript.

**Funding:** This research received no external funding.

**Institutional Review Board Statement:** Not applicable.

**Informed Consent Statement:** Not applicable.

**Data Availability Statement:** Not applicable.

**Acknowledgments:** The authors want to thank the members of the AIMAT-CINCOMINET (Cementitious and Innovative Construction Materials Interdisciplinary Network) group for critical revision of the paper. The AIMAT-CINCOMINET group includes 20 Italian universities involved in research, development and dissemination in the field of traditional and innovative construction materials.

**Conflicts of Interest:** The authors declare no conflict of interest.

## References

1. Wang, S.; Yan, C.; Xiao, F. Quantitative energy performance assessment methods for existing buildings. *Energy Build.* **2012**, *55*, 873–888. [\[CrossRef\]](#)
2. Giosuè, C.; Belli, A.; Mobili, A.; Citterio, B.; Biavasco, F.; Ruello, M.L.; Tittarelli, F. Improving the Impact of Commercial Paint on Indoor Air Quality by Using Highly Porous Fillers. *Buildings* **2017**, *7*, 110. [\[CrossRef\]](#)
3. Coppola, L.; Beretta, S.; Bignozzi, M.C.; Bolzoni, F.; Brenna, A.; Cabrini, M.; Candamano, S.; Caputo, D.; Carsana, M.; Cioffi, R.; et al. The Improvement of Durability of Reinforced Concretes for Sustainable Structures: A Review on Different Approaches. *Materials* **2022**, *15*, 2728. [\[CrossRef\]](#) [\[PubMed\]](#)
4. Sufian Badar, M.; Kupwade-Patil, K.; Bernal, S.A.; Provis, J.L.; Allouche, E.N. Corrosion of steel bars induced by accelerated carbonation in low and high calcium fly ash geopolymer concretes. *Constr. Build. Mater.* **2014**, *61*, 79–89. [\[CrossRef\]](#)
5. Tittarelli, F.; Mobili, A.; Giosuè, C.; Belli, A.; Bellezze, T. Corrosion behaviour of bare and galvanized steel in geopolymer and Ordinary Portland Cement based mortars with the same strength class exposed to chlorides. *Corros. Sci.* **2018**, *134*, 64–77. [\[CrossRef\]](#)
6. Mobili, A.; Giosuè, C.; Tittarelli, F. Valorisation of GRP Dust Waste in Fired Clay Bricks. *Adv. Civ. Eng.* **2018**, *2018*, 5256741. [\[CrossRef\]](#)
7. Mobili, A.; Belli, A.; Giosuè, C.; Telesca, A.; Marroccoli, M.; Tittarelli, F. Calcium Sulfoaluminate, Geopolymeric, and Cementitious Mortars for Structural Applications. *Environments* **2017**, *4*, 64. [\[CrossRef\]](#)
8. Ekolu, S.O. A review on effects of curing, sheltering, and CO<sub>2</sub> concentration upon natural carbonation of concrete. *Constr. Build. Mater.* **2016**, *127*, 306–320. [\[CrossRef\]](#)
9. James, A.; Bazarchi, E.; Chiniforush, A.A.; Panjebashi, P.; Hosseini, M.R.; Akbarnezhad, A.; Martek, I.; Ghodoosi, F. Rebar corrosion detection, protection, and rehabilitation of reinforced concrete structures in coastal environments: A review. *Constr. Build. Mater.* **2019**, *224*, 1026–1039. [\[CrossRef\]](#)
10. Yao, W.; Liu, H.; Xu, Y.; Xia, K.; Zhu, J. Thermal degradation of dynamic compressive strength for two mortars. *Constr. Build. Mater.* **2017**, *136*, 139–152. [\[CrossRef\]](#)



11. De Sitter, W.R. Costs of service life optimization “The Law of Fives”. In Proceedings of the CEB-RILEM Workshop on Durability of Concrete Structures, Copenhagen, Denmark, 18–20 May 1983; Comité Euro-International du Béton: Copenhagen, Denmark, 1984; pp. 131–134.
12. Bertolini, L.; Elsener, B.; Pedferri, P.; Polder, R. *Corrosion of Steel in Concrete: Prevention, Diagnosis, Repair*; Wiley-VCH: Weinheim, Germany, 2004; ISBN 9783527619306.
13. Tuutti, K. *Corrosion of Steel in Concrete*; Swedish Cement and Concrete Research Institute: Stockholm, Sweden, 1982.
14. Bellezze, T.; Barbaresi, E.; Bartolucci, A.; Fratesi, R. Metodo Visivo per la Misura Dell’Avanzamento del Fronte di Carbonatazione Nel Calcestruzzo. Italian Patent 0001429374, 13 April 2015.
15. Bellezze, T.; Barbaresi, E.; Fratesi, R.; Marinelli, U. Monitoring corrosion in concrete by means of electrical resistance probes. In Proceedings of the INTERCORR 2012, Salvador, Brazil, 14–18 May 2012.
16. Shi, X.; Ye, Z.; Muthumani, A.; Zhang, Y.; Dante, J.F.; Yu, H. *A Corrosion Monitoring System for Existing Reinforced Concrete Structures*; Final Report SPR 736; Oregon Department of Transportation Research: Salem, OR, USA, 2015.
17. Tittarelli, F.; Moriconi, G. Sistema di Monitoraggio per la Manutenzione Preventiva e Programmata Delle Strutture in Calcestruzzo Armato. Italian Patent 0001364988, 8 September 2005.
18. Heyse, P.; Buyle, G.; Walendy, B.; Beccarelli, P.; Loriga, G.; Zangani, D. MULTITEXCO-High Performance Smart Multifunctional Technical Textiles for the Construction Sector. *Procedia Eng.* **2015**, *114*, 11–17. [[CrossRef](#)]
19. Feng, D.; Feng, M.Q. Computer vision for SHM of civil infrastructure: From dynamic response measurement to damage detection—A review. *Eng. Struct.* **2018**, *156*, 105–117. [[CrossRef](#)]
20. Jia, Y.; Tang, L.; Ming, P.; Xie, Y. Ultrasound-excited thermography for detecting microcracks in concrete materials. *NDT E Int.* **2019**, *101*, 62–71. [[CrossRef](#)]
21. Cotič, P.; Kolarič, D.; Bosiljkov, V.B.; Bosiljkov, V.; Jagličić, Z. Determination of the applicability and limits of void and delamination detection in concrete structures using infrared thermography. *NDT E Int.* **2015**, *74*, 87–93. [[CrossRef](#)]
22. Azarsa, P.; Gupta, R. Electrical Resistivity of Concrete for Durability Evaluation: A Review. *Adv. Mater. Sci. Eng.* **2017**, *2017*, 8453095. [[CrossRef](#)]
23. EnDurCrete Project. Available online: <http://www.endurcrete.eu/> (accessed on 10 December 2022).
24. Chung, D.D.L. Carbon materials for structural self-sensing, electromagnetic shielding and thermal interfacing. *Carbon* **2012**, *50*, 3342–3353. [[CrossRef](#)]
25. Yıldırım, G.; Öztürk, O.; Al-Dahawi, A.; Afşin Ulu, A.; Şahmaran, M. Self-sensing capability of Engineered Cementitious Composites: Effects of aging and loading conditions. *Constr. Build. Mater.* **2020**, *231*, 117132. [[CrossRef](#)]
26. Mohammed, A.; Sanjayan, J.G.; Duan, W.H.; Nazari, A. Incorporating graphene oxide in cement composites: A study of transport properties. *Constr. Build. Mater.* **2015**, *84*, 341–347. [[CrossRef](#)]
27. Donnini, J.; Bellezze, T.; Corinaldesi, V. Mechanical, electrical and self-sensing properties of cementitious mortars containing short carbon fibers. *J. Build. Eng.* **2018**, *20*, 8–14. [[CrossRef](#)]
28. Chung, D.D.L. Piezoresistive Cement-Based Materials for Strain Sensing. *J. Intell. Mater. Syst. Struct.* **2002**, *13*, 599–609. [[CrossRef](#)]
29. Siddique, R.; Mehta, A. Effect of carbon nanotubes on properties of cement mortars. *Constr. Build. Mater.* **2014**, *50*, 116–129. [[CrossRef](#)]
30. Le, J.-L.; Du, H.; Pang, S.D. Use of 2D Graphene Nanoplatelets (GNP) in cement composites for structural health evaluation. *Compos. Part B Eng.* **2014**, *67*, 555–563. [[CrossRef](#)]
31. Wen, S.; Chung, D.D.L. Partial replacement of carbon fiber by carbon black in multifunctional cement-matrix composites. *Carbon* **2007**, *45*, 505–513. [[CrossRef](#)]
32. D’Alessandro, A.; Coffetti, D.; Crotti, E.; Coppola, L.; Meoni, A.; Ubertini, F. Self-Sensing Properties of Green Alkali-Activated Binders with Carbon-Based Nano-inclusions. *Sustainability* **2020**, *12*, 9916. [[CrossRef](#)]
33. Han, B.G.; Han, B.Z.; Ou, J.P. Experimental study on use of nickel powder-filled Portland cement-based composite for fabrication of piezoresistive sensors with high sensitivity. *Sens. Actuators A Phys.* **2009**, *149*, 51–55. [[CrossRef](#)]
34. Han, B.; Zhang, L.; Zhang, C.; Wang, Y.; Yu, X.; Ou, J. Reinforcement effect and mechanism of carbon fibers to mechanical and electrically conductive properties of cement-based materials. *Constr. Build. Mater.* **2016**, *125*, 479–489. [[CrossRef](#)]
35. Tong, T.; Fan, Z.; Liu, Q.; Wang, S.; Tan, S.; Yu, Q. Investigation of the effects of graphene and graphene oxide nanoplatelets on the micro- and macro-properties of cementitious materials. *Constr. Build. Mater.* **2016**, *106*, 102–114. [[CrossRef](#)]
36. Chuah, S.; Pan, Z.; Sanjayan, J.G.; Wang, C.M.; Duan, W.H. Nano reinforced cement and concrete composites and new perspective from graphene oxide. *Constr. Build. Mater.* **2014**, *73*, 113–124. [[CrossRef](#)]
37. Xie, P.; Gu, P.; Beaudoin, J.J. Electrical percolation phenomena in cement composites containing conductive fibres. *J. Mater. Sci.* **1996**, *31*, 4093–4097. [[CrossRef](#)]
38. Wen, S.; Chung, D.D.L. A comparative study of steel- and carbon-fibre cement as piezoresistive strain sensors. *Adv. Cem. Res.* **2003**, *15*, 119–128. [[CrossRef](#)]
39. Belli, A.; Mobili, A.; Bellezze, T.; Tittarelli, F. Commercial and recycled carbon/steel fibers for fiber-reinforced cement mortars with high electrical conductivity. *Cem. Concr. Compos.* **2020**, *109*, 103569. [[CrossRef](#)]
40. Mobili, A.; Giosuè, C.; Bellezze, T.; Revel, G.M.; Tittarelli, F. Gasification Char and Used Foundry Sand as Alternative Fillers to Graphene Nanoplatelets for Electrically Conductive Mortars with and without Virgin/Recycled Carbon Fibres. *Appl. Sci.* **2021**, *11*, 50. [[CrossRef](#)]

41. Available online: <http://www.esrl.noaa.gov/gmd/ccgg/trends/full.html> (accessed on 8 January 2023).
42. Aggarwal, P.; Aggarwal, Y. Carbonation and corrosion of SCC. In *Self Compacting Concrete: Materials, Properties and Applications*; Siddique, R., Ed.; Woodhead Publishing: Duxford, UK, 2020; pp. 148–149.
43. Lahdensivu, J.; Makela, H.; Pirinen, P. Corrosion of reinforcement in existing concrete facades. In *Durability of Building Materials and Components*; Peixoto de Freitas, V., Costa, A., Delgado, J., Eds.; Springer: Berlin, Germany, 2013; pp. 253–274.
44. Pagliolico, S.L.; Doglione, R.; Tulliani, J.-M. Diagnosis of the surface layer damage in a 1960s reinforced concrete building. *Case Stud. Constr. Mater.* **2014**, *1*, 77–82. [[CrossRef](#)]
45. Montemor, M.F.; Simões, A.M.P.; Ferreira, M.G.S. Chloride-induced corrosion on reinforcing steel: From the fundamentals to the monitoring techniques. *Cem. Concr. Compos.* **2003**, *25*, 491–502. [[CrossRef](#)]
46. Maalej, M.; Ahmed, S.F.U.; Kuang, K.S.C.; Paramasivam, P. Fiber Optic Sensing for Monitoring Corrosion-Induced Damage. *Struct. Heal. Monit.* **2004**, *3*, 165–176. [[CrossRef](#)]
47. Kawasaki, Y.; Tomoda, Y.; Ohtsu, M. AE monitoring of corrosion process in cyclic wet–dry test. *Constr. Build. Mater.* **2010**, *24*, 2353–2357. [[CrossRef](#)]
48. Behnood, A.; Van Tittelboom, K.; De Belie, N. Methods for measuring pH in concrete: A review. *Constr. Build. Mater.* **2016**, *105*, 176–188. [[CrossRef](#)]
49. Mayer, T.; Gehlen, C.; Dauberschmidt, C. Corrosion monitoring in concrete. In *Techniques for Corrosion Monitoring*; Yang, L., Ed.; Woodhead Publishing: Duxford, UK, 2020; pp. 39–405.
50. Seguí Femenias, Y.; Angst, U.; Elsener, B. PH-monitoring in mortar with thermally-oxidized iridium electrodes. *RILEM Tech. Lett.* **2017**, *2*, 59–66. [[CrossRef](#)]
51. Seguí Femenias, Y.; Angst, U.; Elsener, B. Monitoring pH in corrosion engineering by means of thermally produced iridium oxide electrodes. *Mater. Corros.* **2018**, *69*, 76–88. [[CrossRef](#)]
52. Bhadra, S.; Tan, D.S.Y.; Thomson, D.J.; Freund, M.S.; Bridges, G.E. A Wireless Passive Sensor for Temperature Compensated Remote pH Monitoring. *IEEE Sens. J.* **2013**, *13*, 2428–2436. [[CrossRef](#)]
53. Gandía-Romero, J.M.; Campos, I.; Valcuende, M.; García-Breijo, E.; Marcos, M.D.; Payá, J.; Soto, J. Potentiometric thick-film sensors for measuring the pH of concrete. *Cem. Concr. Compos.* **2016**, *68*, 66–76. [[CrossRef](#)]
54. Colozza, N.; Tazzioli, S.; Sassolini, A.; Agosta, L.; di Monte, M.G.; Hermansson, K.; Arduini, F. Multiparametric analysis by paper-assisted potentiometric sensors for diagnostic and monitoring of reinforced concrete structures. *Sens. Actuators B Chem.* **2021**, *345*, 130352. [[CrossRef](#)]
55. Habel, W.R.; Krebber, K. Fiber-optic sensor applications in civil and geotechnical engineering. *Photonic Sens.* **2011**, *1*, 268–280. [[CrossRef](#)]
56. Staneva, D.; Betcheva, R. Synthesis and functional properties of new optical pH sensor based on benzo[de]anthracen-7-one immobilized on the viscose. *Dye. Pigment.* **2007**, *74*, 148–153. [[CrossRef](#)]
57. Xie, W.; Sun, T.; Grattan, K.; McPolin, D.; Basheer, P.; Long, A. Fibre optic chemical sensor systems for internal concrete condition monitoring. In *Proceedings of the Second European Workshop on Optical Fibre Sensors, Santander, Spain, 9–11 June 2004*; pp. 334–337.
58. Grattan, S.; Taylor, S.; Basheer, P.; Sun, T.; Grattan, K. Sensors systems, especially fibre optic sensors in structural monitoring applications in concrete: An overview. In *New Developing in Sensing Technology for Structural Health Monitoring. Lecture Notes in Electrical Engineering*; Mukhopadhyay, S., Ed.; Springer: Berlin, Germany, 2011; pp. 359–425.
59. McPolin, D.O.; Basheer, P.M.; Grattan, K.T.; Long, A.E.; Sun, T.; Xie, W. Preliminary Development and Evaluation of Fiber-Optic Chemical Sensors. *J. Mater. Civ. Eng.* **2011**, *23*, 1200–1210. [[CrossRef](#)]
60. Khalil, G.E.; Daddario, P.; Lau, K.S.F.; Imtiaz, S.; King, M.; Gouterman, M.; Sidelev, A.; Puran, N.; Ghandehari, M.; Brückner, C. meso-Tetraarylporpholactones as high pH sensors. *Analyst* **2010**, *135*, 2125–2131. [[CrossRef](#)]
61. Srinivasan, R.; Phillips, T.; Bargeron, C.; Carlson, M.; Schemm, E.; Saffarian, H. Embedded micro-sensor for monitoring pH in concrete structures. In *Proceedings of the Smart Structures and Materials 2000: Smart Systems for Bridges, Structures, and Highways, Newport Beach, CA, USA, 6–7 March 2000*; pp. 40–44.
62. Inserra, B.; Hayashi, K.; Marchisio, A.; Tulliani, J.-M. Sol–gel-entrapped pH indicator for monitoring pH variations in cementitious materials. *J. Appl. Biomater. Funct. Mater.* **2020**, *18*, 2280800020936540. [[CrossRef](#)]
63. Polder, R.B. Electrochemical techniques for corrosion protection and maintenance. In *Corrosion in Reinforced Concrete Structures*; Woodhead Publishing Limited: Sawston, UK, 2005; pp. 215–241.
64. Redaelli, E.; Carsana, M.; Gastaldi, M.; Lollini, F.; Bertolini, L. Electrochemical techniques for the repair of reinforced concrete suffering carbonation-induced corrosion. *Corros. Rev.* **2011**, *29*, 179–190. [[CrossRef](#)]
65. Pedferri, P. Cathodic protection and cathodic prevention. *Constr. Build. Mater.* **1996**, *10*, 391–402. [[CrossRef](#)]
66. Bertolini, L.; Bolzoni, F.; Cigada, A.; Pastore, T.; Pedferri, P. Cathodic protection of new and old reinforced concrete structures. *Corros. Sci.* **1993**, *35*, 1633–1639. [[CrossRef](#)]
67. Bertolini, L.; Bolzoni, F.; Pedferri, P.; Lazzari, L.; Pastore, T. Cathodic protection and cathodic prevention in concrete: Principles and applications. *J. Appl. Electrochem.* **1998**, *28*, 1321–1331. [[CrossRef](#)]
68. Glass, G.K.; Buenfeld, N.R. Theoretical basis for designing reinforced concrete cathodic protection systems. *Br. Corros. J.* **1997**, *32*, 179–184. [[CrossRef](#)]
69. Glass, G.K. The 100-mV potential decay cathodic protection criterion. *Corrosion* **1999**, *55*, 286–290. [[CrossRef](#)]

70. Bertolini, L.; Pedferri, P.; Redaelli, E.; Pastore, T. Repassivation of steel in carbonated concrete induced by cathodic protection. *Mater. Corros.* **2003**, *54*, 163–175. [[CrossRef](#)]
71. Page, C.L.; Sergi, G. Developments in Cathodic Protection Applied to Reinforced Concrete. *J. Mater. Civ. Eng.* **2000**, *12*, 8–15. [[CrossRef](#)]
72. Redaelli, E.; Lollini, F.; Bertolini, L. Cathodic protection with localised galvanic anodes in slender carbonated concrete elements. *Mater. Struct.* **2014**, *47*, 1839–1855. [[CrossRef](#)]
73. Bertolini, L.; Carsana, M.; Redaelli, E. Conservation of historical reinforced concrete structures damaged by carbonation induced corrosion by means of electrochemical realkalisation. *J. Cult. Herit.* **2008**, *9*, 376–385. [[CrossRef](#)]
74. Bertolini, L.; Lupica Spagnolo, S.; Redaelli, E. Electrochemical Realkalization as a Conservation Technique for Reinforced Concrete. *Int. J. Archit. Herit.* **2012**, *6*, 214–227. [[CrossRef](#)]
75. Redaelli, E.; Bertolini, L. Electrochemical repair techniques in carbonated concrete. Part I: Electrochemical realkalisation. *J. Appl. Electrochem.* **2011**, *41*, 817–827. [[CrossRef](#)]
76. Wang, B.; Zhao, R.; Zhang, T. Pore structure and durability of cement-based composites doped with graphene nanoplatelets. *Mater. Express* **2018**, *8*, 149–156. [[CrossRef](#)]
77. Venugopal, P.; Shekhar, A.; Visser, E.; Scheele, N.; Chandra Mouli, G.R.; Bauer, P.; Silvester, S. Roadway to self-healing highways with integrated wireless electric vehicle charging and sustainable energy harvesting technologies. *Appl. Energy* **2018**, *212*, 1226–1239. [[CrossRef](#)]
78. Liu, Q.; Xu, Q.; Yu, Q.; Gao, R.; Tong, T. Experimental investigation on mechanical and piezoresistive properties of cementitious materials containing graphene and graphene oxide nanoplatelets. *Constr. Build. Mater.* **2016**, *127*, 565–576. [[CrossRef](#)]
79. Zheng, Q.; Han, B.; Cui, X.; Yu, X.; Ou, J. Graphene-engineered cementitious composites. *Nanomater. Nanotechnol.* **2017**, *7*, 184798041774230. [[CrossRef](#)]
80. Bianco, A.; Cheng, H.-M.; Enoki, T.; Gogotsi, Y.; Hurt, R.H.; Koratkar, N.; Kyotani, T.; Monthieux, M.; Park, C.R.; Tascon, J.M.D.; et al. All in the graphene family—A recommended nomenclature for two-dimensional carbon materials. *Carbon* **2013**, *65*, 1–6. [[CrossRef](#)]
81. Wick, P.; Louw-Gaume, A.E.; Kucki, M.; Krug, H.F.; Kostarelos, K.; Fadeel, B.; Dawson, K.A.; Salvati, A.; Vázquez, E.; Ballerini, L.; et al. Classification Framework for Graphene-Based Materials. *Angew. Chemie Int. Ed.* **2014**, *53*, 7714–7718. [[CrossRef](#)]
82. Verdolotti, L.; Santillo, C.; Rollo, G.; Romanelli, G.; Lavorgna, M.; Liguori, B.; Lama, G.C.; Preziosi, E.; Senesi, R.; Andreani, C.; et al. MWCNT/rGO/natural rubber latex dispersions for innovative, piezo-resistive and cement-based composite sensors. *Sci. Rep.* **2021**, *11*, 18975. [[CrossRef](#)]
83. Chougan, M.; Marotta, E.; Lamastra, F.R.; Vivio, F.; Montesperelli, G.; Ianniruberto, U.; Bianco, A. A systematic study on EN-998-2 premixed mortars modified with graphene-based materials. *Constr. Build. Mater.* **2019**, *227*, 116701. [[CrossRef](#)]
84. Yang, H.; Cui, H.; Tang, W.; Li, Z.; Han, N.; Xing, F. A critical review on research progress of graphene/cement based composites. *Compos. Part A Appl. Sci. Manuf.* **2017**, *102*, 273–296. [[CrossRef](#)]
85. Han, B.; Zheng, Q.; Sun, S.; Dong, S.; Zhang, L.; Yu, X.; Ou, J. Enhancing mechanisms of multi-layer graphenes to cementitious composites. *Compos. Part A Appl. Sci. Manuf.* **2017**, *101*, 143–150. [[CrossRef](#)]
86. Dalla, P.; Tragazikis, I.; Exarchos, D.; Dassios, K.; Barkoula, N.; Matikas, T. Effect of Carbon Nanotubes on Chloride Penetration in Cement Mortars. *Appl. Sci.* **2019**, *9*, 1032. [[CrossRef](#)]
87. Xu, Y.; Fan, Y. Effect Of On Graphene Oxide the Concrete Resistance to Chloride Ion Permeability. *IOP Conf. Ser. Mater. Sci. Eng.* **2018**, *394*, 032020. [[CrossRef](#)]
88. Du, H.J.; Pang, S.D. Transport of Water and Chloride Ion in Cement Composites Modified with Graphene Nanoplatelet. *Key Eng. Mater.* **2014**, *629–630*, 162–167. [[CrossRef](#)]
89. Dimov, D.; Amit, I.; Gorrie, O.; Barnes, M.D.; Townsend, N.J.; Neves, A.I.S.; Withers, F.; Russo, S.; Craciun, M.F. Ultrahigh Performance Nanoengineered Graphene-Concrete Composites for Multifunctional Applications. *Adv. Funct. Mater.* **2018**, *28*, 1705183. [[CrossRef](#)]
90. Fadeel, B.; Bussy, C.; Merino, S.; Vázquez, E.; Flahaut, E.; Mouchet, F.; Evariste, L.; Gauthier, L.; Koivisto, A.J.; Vogel, U.; et al. Safety Assessment of Graphene-Based Materials: Focus on Human Health and the Environment. *ACS Nano* **2018**, *12*, 10582–10620. [[CrossRef](#)]
91. Bussy, C.; Ali-Boucetta, H.; Kostarelos, K. Safety Considerations for Graphene: Lessons Learnt from Carbon Nanotubes. *Acc. Chem. Res.* **2013**, *46*, 692–701. [[CrossRef](#)]
92. Nanni, A. A New Tool for Concrete and Masonry Repair. *Concr. Int.* **2012**, *34*, 43–49.
93. Awani, O.; El-Maaddawy, T.; Ismail, N. Fabric-reinforced cementitious matrix: A promising strengthening technique for concrete structures. *Constr. Build. Mater.* **2017**, *132*, 94–111. [[CrossRef](#)]
94. Zhu, Y.; Zhang, Y.; Hussein, H.H.; Chen, G. Flexural strengthening of reinforced concrete beams or slabs using ultra-high performance concrete (UHPC): A state of the art review. *Eng. Struct.* **2020**, *205*, 110035. [[CrossRef](#)]
95. *ACI 549.4R*; Design and Construction of Externally Bonded Fabric-Reinforced Cementitious Matrix (FRCM) Systems for Repair and Strengthening Concrete and Masonry Structures. American Concrete Institute: Farmington Hills, MI, USA, 2013.
96. *CNR-DT 215/2018*; Istruzioni per la Progettazione, l'Esecuzione ed il Controllo di Interventi di Consolidamento Statico Mediante L'utilizzo di Compositi Fibrorinforzati a Matrice Inorganica. National Research Council of Italy: Rome, Italy, 2018.



97. ICC-ES AC434.13; Acceptance Criteria for Masonry and Concrete Strengthening Using Fabric Reinforced Cementitious Matrix (FRCM) Composite Systems. International Code Council: Washington, DC, USA, 2013.
98. Consiglio Superiore dei Lavori Pubblici—Servizio Tecnico Centrale. *Linea Guida per la Identificazione, la Qualificazione ed il Controllo di Accettazione di Compositi Fibrorinforzati a Matrice Inorganica (FRCM) da Utilizzarsi per il Consolidamento Strutt;* Consiglio Superiore dei Lavori Pubblici—Servizio Tecnico Centrale: Rome, Italy, 2018.
99. RILEM TC 250-CSM; Composites for Sustainable Strengthening of Masonry. RILEM: Champs-sur-Marne, France, 2012.
100. Carozzi, F.G.; Bellini, A.; D'Antino, T.; de Felice, G.; Focacci, F.; Hojdys, L.; Laghi, L.; Lanoye, E.; Micelli, F.; Panizza, M.; et al. Experimental investigation of tensile and bond properties of Carbon-FRCM composites for strengthening masonry elements. *Compos. Part B Eng.* **2017**, *128*, 100–119. [[CrossRef](#)]
101. D'Antino, T.; Carloni, C.; Sneed, L.H.; Pellegrino, C. Matrix–fiber bond behavior in PBO FRCM composites: A fracture mechanics approach. *Eng. Fract. Mech.* **2014**, *117*, 94–111. [[CrossRef](#)]
102. D'Ambrisi, A.; Feo, L.; Focacci, F. Experimental and analytical investigation on bond between Carbon-FRCM materials and masonry. *Compos. Part B Eng.* **2013**, *46*, 15–20. [[CrossRef](#)]
103. Bompadre, F.; Donnini, J. Surface modification of glass textile for the reinforcement of a cement-based composite: A review. *Appl. Sci.* **2021**, *11*, 2028. [[CrossRef](#)]
104. Babaeidarabad, S.; Arboleda, D.; Loreto, G.; Nanni, A. Shear strengthening of un-reinforced concrete masonry walls with fabric-reinforced-cementitious-matrix. *Constr. Build. Mater.* **2014**, *65*, 243–253. [[CrossRef](#)]
105. Mazzotti, C.; Ferretti, F.; Ferracuti, B.; Incerti, A. Diagonal compression tests on masonry panels strengthened by FRP and FRCM. In *Structural Analysis of Historical Constructions: Anamnesis, Diagnosis, Therapy, Controls*; CRC Press: Boca Raton, FL, USA, 2016; pp. 1069–1076. [[CrossRef](#)]
106. Gattesco, N.; Boem, I.; Dudine, A. Diagonal compression tests on masonry walls strengthened with a GFRP mesh reinforced mortar coating. *Bull. Earthq. Eng.* **2015**, *13*, 1703–1726. [[CrossRef](#)]
107. Koutas, L.N.; Tetta, Z.; Bournas, D.A.; Triantafillou, T.C. Strengthening of Concrete Structures with Textile Reinforced Mortars: State-of-the-Art Review. *J. Compos. Constr.* **2019**, *23*, 03118001. [[CrossRef](#)]
108. Escrig, C.; Gil, L.; Bernat-Maso, E.; Puigvert, F. Experimental and analytical study of reinforced concrete beams shear strengthened with different types of textile-reinforced mortar. *Constr. Build. Mater.* **2015**, *83*, 248–260. [[CrossRef](#)]
109. Donnini, J. Durability of glass FRCM systems: Effects of different environments on mechanical properties. *Compos. Part B Eng.* **2019**, *174*, 107047. [[CrossRef](#)]
110. Nobili, A.; Signorini, C. On the effect of curing time and environmental exposure on impregnated Carbon Fabric Reinforced Cementitious Matrix (CFRCM) composite with design considerations. *Compos. Part B Eng.* **2017**, *112*, 300–313. [[CrossRef](#)]
111. Pekmezci, B.Y.; Arabaci, E.; Ustundag, C. Freeze-thaw durability of lime based FRCM systems for strengthening historical masonry. In *Key Engineering Materials*; Trans Tech Publications Ltd.: Wollerau, Switzerland, 2019.
112. Franzoni, E.; Gentilini, C.; Santandrea, M.; Carloni, C. Effects of rising damp and salt crystallization cycles in FRCM-masonry interfacial debonding: Towards an accelerated laboratory test method. *Constr. Build. Mater.* **2018**, *175*, 225–238. [[CrossRef](#)]
113. Bompadre, F.; Donnini, J. Fabric-Reinforced Cementitious Matrix (FRCM) Carbon Yarns with Different Surface Treatments Embedded in a Cementitious Mortar: Mechanical and Durability Studies. *Materials* **2022**, *15*, 3927. [[CrossRef](#)]
114. Bisby, L. Fire Resistance of Textile Fiber Composites Used in Civil Engineering. In *Textile Fibre Composites in Civil Engineering*; Woodhead Publishing: Sawston, UK, 2016; pp. 169–185; ISBN 9781782424697.
115. Michels, J.; Zwicky, D.; Scherer, J.; Harmanci, Y.E.; Motavalli, M. Structural Strengthening of Concrete with Fiber Reinforced Cementitious Matrix (FRCM) at Ambient and Elevated Temperature—Recent Investigations in Switzerland. *Adv. Struct. Eng.* **2014**, *17*, 1785–1799. [[CrossRef](#)]
116. Consiglio Superiore dei Lavori Pubblici—Servizio Tecnico Centrale. *Linea Guida per la Identificazione, la Qualificazione ed il Controllo di Fibrorinforzati a Matrice Polimerica da Utilizzarsi per il Consolidamento Strutturale di Costruzioni Esistenti con la Tecnica Dell'intonaco Armato CRM*; Consiglio Superiore dei Lavori Pubblici—Servizio Tecnico Centrale: Rome, Italy, 2019; pp. 1–38.
117. D'Antino, T.; Carozzi, F.G.; Poggi, C. Diagonal shear behavior of historic walls strengthened with composite reinforced mortar (CRM). *Mater. Struct. Constr.* **2019**, *52*, 114. [[CrossRef](#)]
118. Donnini, J.; Maracchini, G.; Lenci, S.; Corinaldesi, V.; Quagliarini, E. TRM reinforced tuff and fired clay brick masonry: Experimental and analytical investigation on their in-plane and out-of-plane behavior. *Constr. Build. Mater.* **2021**, *272*, 121643. [[CrossRef](#)]
119. De Santis, S.; de Felice, G. Shake table tests on a tuff masonry structure strengthened with composite reinforced mortar. *Compos. Struct.* **2021**, *275*, 114508. [[CrossRef](#)]
120. Del Zoppo, M.; Di Ludovico, M.; Balsamo, A.; Prota, A. In-plane shear capacity of tuff masonry walls with traditional and innovative Composite Reinforced Mortars (CRM). *Constr. Build. Mater.* **2019**, *210*, 289–300. [[CrossRef](#)]
121. Wille, K.; El-Tawil, S.; Naaman, A.E. Properties of strain hardening ultra high performance fiber reinforced concrete (UHP-FRC) under direct tensile loading. *Cem. Concr. Compos.* **2014**, *48*, 53–66. [[CrossRef](#)]
122. Naaman, A.E.; Reinhardt, H.W. Proposed classification of HPCFRP composites based on their tensile response. *Mater. Struct. Constr.* **2006**, *39*, 547–555. [[CrossRef](#)]
123. Vicenzino, E.; Cuiham, G.; Perry, V.H.; Zakariasen, D.; Chow, T.S. First Use of UHPFRC in Thin Precast Concrete Roof Shell for Canadian LRT Station. *PCI J.* **2005**, *50*, 50–67. [[CrossRef](#)]



124. Farzad, M.; Shafieifar, M.; Azizinamini, A. Experimental and numerical study on an innovative sandwich system utilizing UPFRC in bridge applications. *Eng. Struct.* **2019**, *180*, 349–356. [[CrossRef](#)]
125. Raza, S.; Khan, M.K.I.; Menegon, S.J.; Tsang, H.-H.; Wilson, J.L. Strengthening and Repair of Reinforced Concrete Columns by Jacketing: State-of-the-Art Review. *Sustainability* **2019**, *11*, 3208. [[CrossRef](#)]
126. Koo, I.Y.; Hong, S.G. Strengthening RC columns with ultra high performance concrete. In Proceedings of the 2016 Structures Congress (Structures16), Jeju Island, Republic of Korea, 28 August–1 September 2016.
127. Meda, A.; Mostosi, S.; Rinaldi, Z.; Riva, P. Corroded RC columns repair and strengthening with high performance fiber reinforced concrete jacket. *Mater. Struct.* **2016**, *49*, 1967–1978. [[CrossRef](#)]
128. Cho, C.-G.; Kim, Y.-Y.; Feo, L.; Hui, D. Cyclic responses of reinforced concrete composite columns strengthened in the plastic hinge region by HPPFRC mortar. *Compos. Struct.* **2012**, *94*, 2246–2253. [[CrossRef](#)]
129. Corinaldesi, V.; Donnini, J.; Nardinocchi, A. The influence of calcium oxide addition on properties of fiber reinforced cement-based composites. *J. Build. Eng.* **2015**, *4*, 14–20. [[CrossRef](#)]
130. Wille, K.; Kim, D.J.; Naaman, A.E. Strain-hardening UHP-FRC with low fiber contents. *Mater. Struct. Constr.* **2011**, *44*, 583–598. [[CrossRef](#)]
131. Yoo, D.-Y.; Banthia, N. Mechanical and structural behaviors of ultra-high-performance fiber-reinforced concrete subjected to impact and blast. *Constr. Build. Mater.* **2017**, *149*, 416–431. [[CrossRef](#)]
132. Máca, P.; Sovják, R.; Konvalinka, P. Mix design of UHPFRC and its response to projectile impact. *Int. J. Impact Eng.* **2014**, *63*, 158–163. [[CrossRef](#)]
133. Yoo, D.-Y.; Kang, S.-T.; Yoon, Y.-S. Effect of fiber length and placement method on flexural behavior, tension-softening curve, and fiber distribution characteristics of UHPFRC. *Constr. Build. Mater.* **2014**, *64*, 67–81. [[CrossRef](#)]
134. AFGC. Setra Working Group Ultra High Performance Fibre-Reinforced Concrete-Interim Recommendations. In Proceedings of the International Conference on the Design and Dynamic Behaviour of Footbridges, Paris, France, 20–22 November 2002.
135. Japan Society of Civil Engineers. *Recommendations for Design and Construction of High Performance Fiber Reinforced Cement Composites with Multiple Fine Cracks (HPPFRC)*; Japan Society of Civil Engineers: Tokyo, Japan, 2008.
136. Sánchez, M.; Faria, P.; Ferrara, L.; Horszczaruk, E.; Jonkers, H.M.; Kwiecień, A.; Mosa, J.; Peled, A.; Pereira, A.S.; Snoeck, D.; et al. External treatments for the preventive repair of existing constructions: A review. *Constr. Build. Mater.* **2018**, *193*, 435–452. [[CrossRef](#)]
137. Pakravan, H.R.; Ozbakkaloglu, T. Synthetic fibers for cementitious composites: A critical and in-depth review of recent advances. *Constr. Build. Mater.* **2019**, *207*, 491–518. [[CrossRef](#)]
138. Yin, S.; Tuladhar, R.; Shi, F.; Combe, M.; Collister, T.; Sivakugan, N. Use of macro plastic fibres in concrete: A review. *Constr. Build. Mater.* **2015**, *93*, 180–188. [[CrossRef](#)]
139. Coppola, B.; Scarfato, P.; Incarnato, L.; Maio, L. Di Durability and mechanical properties of nanocomposite fiber reinforced concrete. *CSE City Saf. Energy* **2014**, *2*, 127–136. [[CrossRef](#)]
140. Lee, S.J.; Won, J.P. Flexural behavior of precast reinforced concrete composite members reinforced with structural nano-synthetic and steel fibers. *Compos. Struct.* **2014**, *118*, 571–579. [[CrossRef](#)]
141. Lee, S.J.; Won, J.P. Interfacial phenomena in structural polymeric nano-clay synthetic fiber reinforced cementitious composites. *Compos. Struct.* **2015**, *133*, 62–69. [[CrossRef](#)]
142. Coppola, B.; Scarfato, P.; Incarnato, L.; Di Maio, L. Morphology development and mechanical properties variation during cold-drawing of polyethylene-clay nanocomposite fibers. *Polymers* **2017**, *9*, 235. [[CrossRef](#)]
143. Coppola, B.; Di Maio, L.; Scarfato, P.; Incarnato, L. Use of polypropylene fibers coated with nano-silica particles into a cementitious mortar. In Proceedings of the AIP Conference Proceedings, Solo, Indonesia, 4–5 November 2015; American Institute of Physics Inc.: College Park, MD, USA, 2015; Volume 1695.
144. Coppola, B.; Di Maio, L.; Courard, L.; Scarfato, P.; Incarnato, L. Use of foamed polypropylene fibers to improve fiber/matrix bond for cementitious composites. In Proceedings of the 20th International Conference on Composite Materials in Copenhagen, Copenhagen, Denmark, 19–24 July 2015.
145. Ferrara, G.; Coppola, B.; Di Maio, L.; Incarnato, L.; Martinelli, E. Tensile strength of flax fabrics to be used as reinforcement in cement-based composites: Experimental tests under different environmental exposures. *Compos. Part B Eng.* **2019**, *168*, 511–523. [[CrossRef](#)]
146. Dittenber, D.B.; Gangarao, H.V.S. Critical review of recent publications on use of natural composites in infrastructure. *Compos. Part A Appl. Sci. Manuf.* **2012**, *43*, 1419–1429. [[CrossRef](#)]
147. Sedan, D.; Pagnoux, C.; Smith, A.; Chotard, T. Mechanical properties of hemp fibre reinforced cement: Influence of the fibre/matrix interaction. *J. Eur. Ceram. Soc.* **2008**, *28*, 183–192. [[CrossRef](#)]
148. Candamano, S.; Crea, F.; Coppola, L.; De Luca, P.; Coffetti, D. Influence of acrylic latex and pre-treated hemp fibers on cement based mortar properties. *Constr. Build. Mater.* **2021**, *273*, 121720. [[CrossRef](#)]
149. Ralegaonkar, R.; Gavali, H.; Aswath, P.; Abolmaali, S. Application of chopped basalt fibers in reinforced mortar: A review. *Constr. Build. Mater.* **2018**, *164*, 589–602. [[CrossRef](#)]
150. Yin, S.; Tuladhar, R.; Shanks, R.A.; Collister, T.; Combe, M.; Jacob, M.; Tian, M.; Sivakugan, N. Fiber preparation and mechanical properties of recycled polypropylene for reinforcing concrete. *J. Appl. Polym. Sci.* **2015**, *132*. [[CrossRef](#)]

151. Won, J.-P.; Park, C.-G.; Lee, S.-J.; Kang, J.-W. Bonding characteristics of recycled polyethylene terephthalate (PET) fibers coated with maleic anhydride grafted polypropylene in cement-based composites. *J. Appl. Polym. Sci.* **2011**, *121*, 1908–1915. [[CrossRef](#)]
152. Aldahdooh, M.A.A.; Jamrah, A.; Alnuaimi, A.; Martini, M.I.; Ahmed, M.S.R.; Ahmed, A.S.R. Influence of various plastics-waste aggregates on properties of normal concrete. *J. Build. Eng.* **2018**, *17*, 13–22. [[CrossRef](#)]
153. Siddique, R.; Khatib, J.; Kaur, I. Use of recycled plastic in concrete: A review. *Waste Manag.* **2008**, *28*, 1835–1852. [[CrossRef](#)] [[PubMed](#)]
154. Iucolano, F.; Liguori, B.; Colella, C. Fibre-reinforced lime-based mortars: A possible resource for ancient masonry restoration. *Constr. Build. Mater.* **2013**, *38*, 785–789. [[CrossRef](#)]
155. Coppola, B.; Palmero, P.; Montanaro, L.; Tulliani, J.M. Alkali-activation of marble sludge: Influence of curing conditions and waste glass addition. *J. Eur. Ceram. Soc.* **2020**, *40*, 3776–3787. [[CrossRef](#)]
156. Bassani, M.; Tefa, L.; Coppola, B.; Palmero, P. Alkali-activation of aggregate fines from construction and demolition waste: Valorisation in view of road pavement subbase applications. *J. Clean. Prod.* **2019**, *234*, 71–84. [[CrossRef](#)]
157. Colangelo, F.; Cioffi, R.; Liguori, B.; Iucolano, F. Recycled polyolefins waste as aggregates for lightweight concrete. *Compos. Part B Eng.* **2016**, *106*, 234–241. [[CrossRef](#)]
158. Coppola, B.; Courard, L.; Michel, F.; Incarnato, L.; Di Maio, L. Investigation on the use of foamed plastic waste as natural aggregates replacement in lightweight mortar. *Compos. Part B Eng.* **2016**, *99*, 75–83. [[CrossRef](#)]
159. Coppola, B.; Courard, L.; Michel, F.; Incarnato, L.; Scarfato, P.; Di Maio, L. Hygro-thermal and durability properties of a lightweight mortar made with foamed plastic waste aggregates. *Constr. Build. Mater.* **2018**, *170*, 200–206. [[CrossRef](#)]
160. Latroch, N.; Benosman, A.S.; Bouhamou, N.E.; Senhadji, Y.; Mouli, M. Physico-mechanical and thermal properties of composite mortars containing lightweight aggregates of expanded polyvinyl chloride. *Constr. Build. Mater.* **2018**, *175*, 77–87. [[CrossRef](#)]
161. Coppola, L.; Coffetti, D.; Crotti, E.; Marini, A.; Passoni, C.; Pastore, T. Lightweight cement-free alkali-activated slag plaster for the structural retrofit and energy upgrading of poor quality masonry walls. *Cem. Concr. Compos.* **2019**, *104*, 103341. [[CrossRef](#)]
162. Singh, H.; Gupta, R. Cellulose fiber as bacteria-carrier in mortar: Self-healing quantification using UPV. *J. Build. Eng.* **2020**, *28*, 101090. [[CrossRef](#)]
163. Liu, J.; Shi, C.; Ma, X.; Khayat, K.H.; Zhang, J.; Wang, D. An overview on the effect of internal curing on shrinkage of high performance cement-based materials. *Constr. Build. Mater.* **2017**, *146*, 702–712. [[CrossRef](#)]
164. Yesilata, B.; Isiker, Y.; Turgut, P. Thermal insulation enhancement in concretes by adding waste PET and rubber pieces. *Constr. Build. Mater.* **2009**, *23*, 1878–1882. [[CrossRef](#)]
165. Corinaldesi, V.; Mazzoli, A.; Moriconi, G. Mechanical behaviour and thermal conductivity of mortars containing waste rubber particles. *Mater. Des.* **2011**, *32*, 1646–1650. [[CrossRef](#)]
166. Saxena, R.; Siddique, S.; Gupta, T.; Sharma, R.K.; Chaudhary, S. Impact resistance and energy absorption capacity of concrete containing plastic waste. *Constr. Build. Mater.* **2018**, *176*, 415–421. [[CrossRef](#)]
167. Langan, B.W.; Weng, K.; Ward, M.A. Effect of silica fume and fly ash on heat of hydration of Portland cement. *Cem. Concr. Res.* **2002**, *32*, 1045–1051. [[CrossRef](#)]
168. Uzal, B.; Turanlı, L.; Yücel, H.; Göncüoğlu, M.C.; Çulfaz, A. Pozzolanic activity of clinoptilolite: A comparative study with silica fume, fly ash and a non-zeolitic natural pozzolan. *Cem. Concr. Res.* **2010**, *40*, 398–404. [[CrossRef](#)]
169. Hekal, E. Effect of some admixtures on the hydration of silica fume and hydrated lime. *J. Mater. Sci. Technol.* **2000**, *16*, 375–378.
170. Malhotra, V.M.; Mehta, P.K. *Pozzolanic and Cementitious Materials*; Gordon and Breach Publishers: Abingdon, UK, 1996.
171. Taylor, H.F.W. *Cement Chemistry*; Thomas Telford Publishing: London, UK, 1997; ISBN 0727725920.
172. Volpe, R.; Taglieri, G.; Daniele, V.; Del Re, G. A Process for the Synthesis of Ca(OH)<sub>2</sub> Nanoparticles by Means of Ionic Exchange Resins. European Patent EP2880101, 12 December 2016.
173. Taglieri, G.; Daniele, V.; Del Re, G.; Volpe, R. A New and Original Method to Produce Ca(OH)<sub>2</sub> Nanoparticles by Using an Anion Exchange Resin. *Adv. Nanoparticles* **2015**, *4*, 17–24. [[CrossRef](#)]
174. Taglieri, G.; Felice, B.; Daniele, V.; Volpe, R.; Mondelli, C. Analysis of the carbonatation process of nanosized Ca(OH)<sub>2</sub> particles synthesized by exchange ion process. *Proc. Inst. Mech. Eng. Part N J. Nanomater. Nanoeng. Nanosyst.* **2016**, *230*, 25–31. [[CrossRef](#)]
175. Taglieri, G.; Daniele, V.; Macera, L.; Mondelli, C. Nano Ca(OH)<sub>2</sub> synthesis using a cost-effective and innovative method: Reactivity study. *J. Am. Ceram. Soc.* **2017**, *100*, 5766–5778. [[CrossRef](#)]
176. Taglieri, G.; Daniele, V.; Macera, L. Synthesizing Alkaline Earth Metal Hydroxides Nanoparticles through an Innovative, Single-Step and Eco-Friendly Method. *Solid State Phenom.* **2019**, *286*, 3–14. [[CrossRef](#)]

**Disclaimer/Publisher's Note:** The statements, opinions and data contained in all publications are solely those of the individual author(s) and contributor(s) and not of MDPI and/or the editor(s). MDPI and/or the editor(s) disclaim responsibility for any injury to people or property resulting from any ideas, methods, instructions or products referred to in the content.